EEET ECOLOGICAL ENGINEERING & ENVIRONMENTAL TECHNOLOGY

Ecological Engineering & Environmental Technology 2023, 24(7), 208–215
https://doi.org/10.12912/27197050/169530
ISSN 2719-7050, License CC-BY 4.0

Received: 2023.07.05
Accepted: 2023.07.19
Published: 2023.08.15

Evaluation of Normalized Difference Vegetation Index by Remote Sensing with Landsat Satellites in the Tayacaja Valley in the Central Andes of Peru

Hipólito Carbajal-Morán[1*], Javier F. Márquez-Camarena[1], Carlos A. Galván-Maldonado[1], Rosa H. Zárate-Quiñones[2], Alberto C. Galván-Maldonado[3], Rossibel J. Muñoz-De la Torre[4]

[1] Instituto de Investigación de Ciencias de Ingeniería, Facultad de Ingeniería Electrónica-Sistemas, Universidad Nacional de Huancavelica, Jr. La Mar 755, Pampas 09156, Huancavelica, Perú

[2] Facultad de Ciencias Forestales y del Ambiente, Universidad Nacional del Centro del Perú, Av. Mariscal Castilla N° 3909-4089, Huancayo 12006, Junín, Perú

[3] Facultad de Ingeniería, Universidad Nacional de Trujillo, VXM5+HVJ, Trujillo 13011, La Libertad, Perú

[4] Facultad de Ciencias de la Salud, Universidad Nacional de Huancavelica, Av. Agricultura Nº 319–321. Sector Paturpampa 09001, Huancavelica, Perú

* Corresponding author's e-mail: hipolito.carbajal@unh.edu.pe

ABSTRACT

The research sought to evaluate the normalized difference vegetation index (NDVI) of the study area located in the province of Tayacaja, which includes the districts of Acraquia, Ahuaycha, Pampas and Daniel Hernández, which is part of the central Andes of Peru. The data were collected in low water seasons with a longitudinal cut of 30 years with one sample per year, starting in 1993 until 2022; these samples corresponded to the month of August of each year. The images were extracted from maps from Landsat satellite databases, which were filtered for low cloud cover to avoid interference with the images. Maps from 1993 to 2012 were obtained from Landsat 5 satellite, while from 2013 to 2022 data were obtained from Landsat 8 satellite. The normalized difference vegetation index was determined using Quantum GIS based on the red and near infrared maps; being the minimum NDVI value obtained -0.18, which corresponds to the aquatic body of the Upamayu River that crosses from west to east the study area; while the highest NDVI obtained was 0.79 indicating a greater vegetation cover constituted by mainly eucalyptus plants. The mean NDVI of the 30 years is close to 0.21; this is an indicator that the vegetation is scarce and that it is decreasing mainly due to population growth.

Keywords: vegetation, satellites, greenness, raster, desertification.

INTRODUCTION

Vegetation indices are used as quantitative indicators of the ecosystem as it involves the greenness of plants, bare soil and the presence of water based on remote data obtained with sensors mounted on platforms such as satellite ones (Rahman & Lamb, 2017); this is possible due to the absorption and reflection characteristics of the ecosystem; NDVI in particular is affected by vegetation (Spadoni et al., 2020). Vegetation covers are different and dependent on changes in environmental parameters and anthropogenic pressures; therefore, it is important to monitor population growth and dependence on vegetation cover (Kasoro et al., 2021).

Remote sensing by multispectral satellites provides valuable data that allow dynamic assessment of land use changes and land cover analysis in the world (Xu et al., 2020). The data provided by remote sensing satellites are of the spatial type, which presents the distribution of elements in

space; spectral, which presents surface features; and temporal, which allows relating variations of areas over time (Dutta et al., The spectral analysis of vegetation cover has been the basis for obtaining different indexes based on relating bands of spectra, these are called vegetation spectral indexes (Ramos et al., 2020), which are calculated from the mathematical combination of two or more bands of a multispectral satellite image and tend to present, in a sharper way, the characteristics of vegetation in isolation from other covers (Radočaj et al., 2023).

The index based on spectra widely used for the determination of plant cover parameters is the NDVI (Huang et al., 2021; Lacouture et al., 2020). The formula that normalizes the differences between red reflectance is centered at 670 nm and near infrared is centered at 860 nm, which correspond to regions of higher reflectance and absorption of plant chlorophyll. NDVI values range from -1 to 1; values less than zero correspond to water bodies; values around zero correspond to bare soil, snow or concrete cover, while positive values correspond to areas with vegetation cover (Fung & Siu, 2000). Vegetation cover presents indices of 0.2–0.8; tropical forests present indices higher than these. NDVI represents the photosynthetic activity of vegetation, being associated with biomass, water stress, carbon accumulation and biodiversity of different ecosystems (Jia et al., 2023; Oddi et al., 2022). The calculation of NDVI makes it possible to track the changes that occur in the terrestrial ecosystem as a result of population increase and anthropogenic activities mainly (Guo et al., 2021).

Recent research has taken advantage of remote sensing and NDVI techniques to characterize the behavior of vegetation cover and the impact of climate change over time; Fokeng & Fogwe (2022) studied the dynamics of vegetation degradation over a 37-year period based on Landsat data and its response to atmospheric variability and human-induced factors in the Bui Plateau of southern Cameroon. Likewise, Meng et al. (2023) analyzed the impacts of climate change and human activities on the NDVI of desert areas in northern China between 2001 and 2020; for which they used the Moderate Resolution Imaging Spectroradiometer (MODIS-NDVI), determining that the role of anthropogenic activities was responsible for more than 70% of the changes, demonstrating that these activities are one of the main factors that cause the variation of NDVI. It is also possible to study spatiotemporal seasonal changes in NDVI, as is the case of the study by Li et al. (2023) where they analyzed NDVI in relation to driving forces in the Wuliangsu Lake basin, northern China, from 1990 to 2020, determining that changes in grasslands and forests were vulnerable to climate change and anthropogenic activities. Cacilda-André et al. (2023) developed a multispectral analysis of Landsat images quantifying coverage changes from 2013 to 2019 in Cuanza-Sul Angola, with the results being severe impacts caused to the environment by human activity in this area and propose mitigation and restoration actions in affected areas.

In Peru, few investigations take advantage of data from satellites used as remote sensing devices. Camas-Guardamino & Mamani-Sinche (2022) evaluated the vegetation and soil saturation in the Regional Conservation Area Humedales de Ventanilla by remote sensing in Peru, in the period 2006 - 2021, demonstrating that the variation of vegetation and soil saturation by remote sensing tools point to a possible eutrophication process which demands more effort for the conservation of this ecosystem. Reymundo & Acevedo (2020) in the study of surface temperature and vegetation condition of the Polylepis forest, district of San Marcos de Rocchac, Tayacaja - Peru, used 9 satellite maps of the Landsat 8 OLI/TIRS satellite, evaluating these NDVI variables confirmed the influence of surface temperature on the health of the vegetation within the forest over time. On the other hand, this work was based on the need to know the behavior of the NDVI from 1993 to 2022 in the valley located in the province of Tayacaja-Huancavelica-Peru; therefore, a spectral analysis of the red and near infrared signals was made, performing a raster calculation using the difference between the reflectance of the bands: 4 corresponding to near infrared and 3 corresponding to visible red for maps coming from Landsat 5; and bands: 5 corresponding to near infrared and 4 corresponding to visible red for maps coming from Landsat 8.

MATERIALS AND METHODS

As materials that allowed the development of the work, we have the maps of the visible red and near infrared spectra stored in the

EarthExplorer database (USGS, 2021). Also used was the freely distributed software QGIS V30 ‘s-Hertogenbosch of 2023, which is an open-source geographic information system (GIS) for different platforms such as GNU/Linux, Microsoft Windows, Android and others. It was developed by OSGeo and officially came into use in 2008; it allows the use of raster and vector formats through the GDAL library (GADL/OGR), also large databases, so in this work it made possible the rasterization of the images obtained. In this work we used Landsat 5 map images; this was developed by NASA, it was put into orbit on March 1, 1984, at 705 km from the Earth, it circled the Earth every 99 minutes and carried the following instruments: Multispectral Scanner (MSS) and Thematic Mapper (TM); this satellite stored image data from different places on Earth for almost 29 years, being a world record as the longest operating Earth observation satellite in history, it was decommissioned in 2013. The data recorded in Landsat 5 by the multispectral scanner (MSS) were used in this work, whose bands are four: band 4 corresponds to visible green with wavelength from 0.5 to 0.6 µm, band 5 corresponds to visible red with wavelength from 0.6 to 0.7 µm, band 6 corresponds to near infrared with wavelength 0.7 to 0.8 µm and band 7 corresponds to near infrared with wavelength from 0.8 to 1.1 µm. On the other hand, Landsat 8 satellite was put into orbit in 2013; this satellite was implemented with Operational Land Imager (OLI) and thermal infrared sensor (TIRS) as main instruments (USGS, 2023a).

Landsat 8 images have 15-meter panchromatic and 30-meter multispectral spatial resolutions along its orbit 185 km from Earth; it contains nine spectral bands: band 1 with wavelengths from 0.43 to 0. 45 µm with 30 m spatial resolution, band 2 blue with wavelength 0.450 to 0.51 µm with 30 m spatial resolution, band 3 green with wavelength 0.53 to 0.59 µm with 30 m spatial resolution, band 4 red with wavelength 0.64 to 0.67 µm with 30 m spatial resolution, band 5 near infrared with wavelength 0.85 to 0.88 µm with 30 m spatial resolution, band 6 SWIR 1 with wavelength 1.57 to 1.65 µm with 30 m spatial resolution, band 7 SWIR 2 with wavelength 2. 11 to 2.29 µm with 30 m spatial resolution, band 8 panchromatic (PAN) with wavelength 0.50 to 0.68 µm with 15 m spatial resolution and band 9 cirrus with wavelength 1.36 to 1.38 µm with 30 m spatial resolution. The Landsat 8 thermal infrared sensor (TIRS) has two spectral bands: band 10 TIRS 1 with wavelength 10.6 to 11.19 µm with 100 m spatial resolution and band 11 TIRS 2 with wavelength 11.5 to 12.51 µm with 100 m spatial resolution (USGS, 2023b). The data were collected according to the territorial demarcation of the Pampas-Tayacaja valley, this collection was made from the Landsat satellite database, for the zone path: 6, row: 69; Figure 1 shows the view of the study area located in the central Andes of Peru, for the year 1993 month of August using Landsat 5, in the same way we proceeded with the use of Landsat 8. The work began by obtaining Landsat maps of the study area for the path: 6, row: 69 satellite zone in true color (see Figure 2) for the 30 years.

The red spectrum map together with the infrared spectrum map was downloaded from

Figure 1. Localized view of the study area with Landsat 5 for satellite zone path: 6, row: 69, obtained with science for a changing world (USGS, 2020)

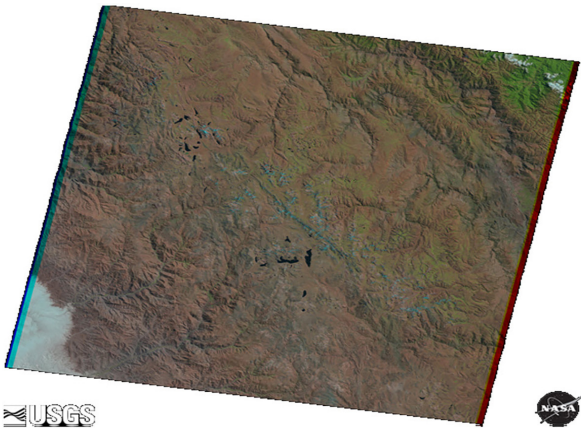

Figure 2. True color map of the study area in satellite zone path: 6, row: 69

EarthExplorer (see Figure 3) which should be identified by bands in both Landsat 5 and Landsat 8. In Landsat 5: band 3 corresponds to red and band 4 to infrared. While in Landsat 8: band 4 corresponds to red and band 5 corresponds to the infrared spectrum. The NDVI was calculated with Equation 1, relating the red and infrared spectra for each map acquired, allowing the rasterization of the images

$$NDVI = (Infrared - Red)/(Infrared + Red) \quad (1)$$

In Figure 4, the NDVI raster band of the study area is calculated with QGIS based on Eq. 1. The result of the NDVI calculation is presented in Figure 5, where the concentration of vegetation cover is shown in green

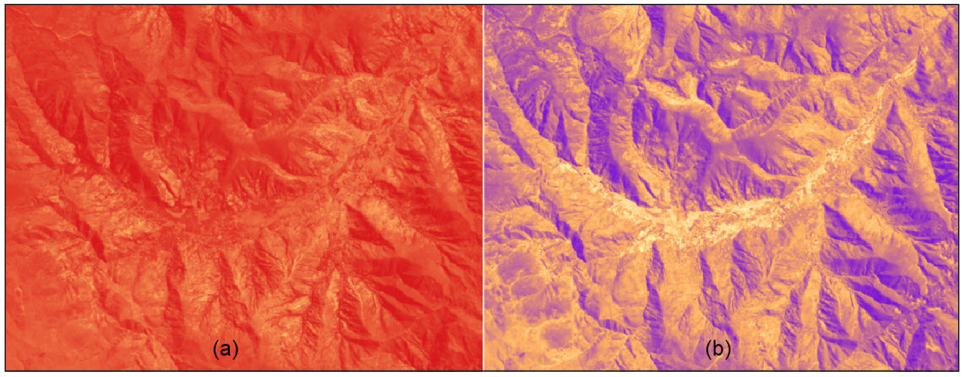

Figure 3. Maps (a) in the red spectrum and (b) in the infrared spectrum corresponding to the study area

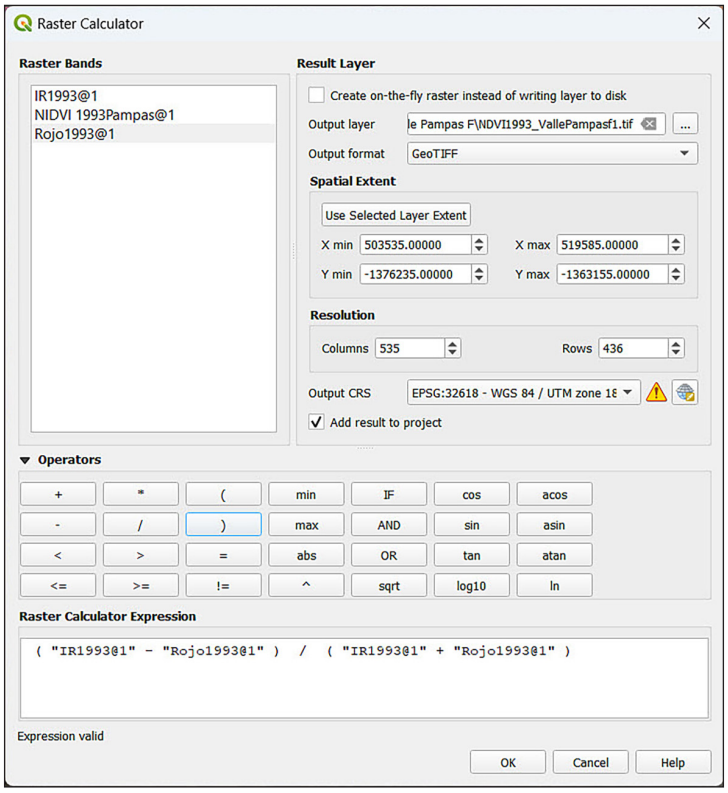

Figure 4. NDVI raster band calculation of the study area with QGIS

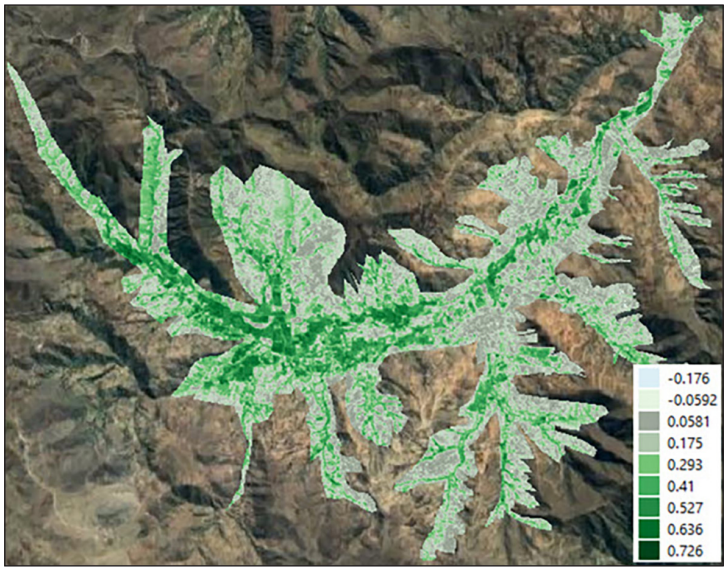

Figure 5. NDVI of the study area obtained by processing in QGIS

RESULTS AND DISCUSSION

As a result of the analysis of the red and infrared spectrum maps, applying equation 1, the NDVI statistical values were rasterized from 1993 to 2022, these values are presented in Table 1; for the years 1993–2012 the NDVI were obtained with Landsat 5 data and for the years 2013–2022 they were obtained with Landsat 8 data, each satellite has a band assigned to the different spectra, which was considered for the rasterization.

The minimum NDVI value obtained was -0.18; this negative value corresponds to the Upamayu water body that crosses the valley from west to east (Carbajal et al., 2021), having a low flow due to the low water season when the study was carried out. The maximum NDVI value was 0.79; this value represents various zones with vegetation cover consisting of eucalyptus trees. The average NDVI obtained from the 30-year longitudinal study was 0.21, which represents overall sparse vegetation. In addition, the green line in Figure 6 indicates that the vegetation is decreasing, limiting the study to the dry season, which corresponds to the months of August.

From the results, the study area in the Tayacaja valley, located in the central Andes of Peru, is located in the Pacific slope zone (GOREH, 2007), so vegetation is scarce, presenting an average NDVI of 0. 21 in the analysis conducted over 30 years, this index which is used to estimate the quantity, quality and development of

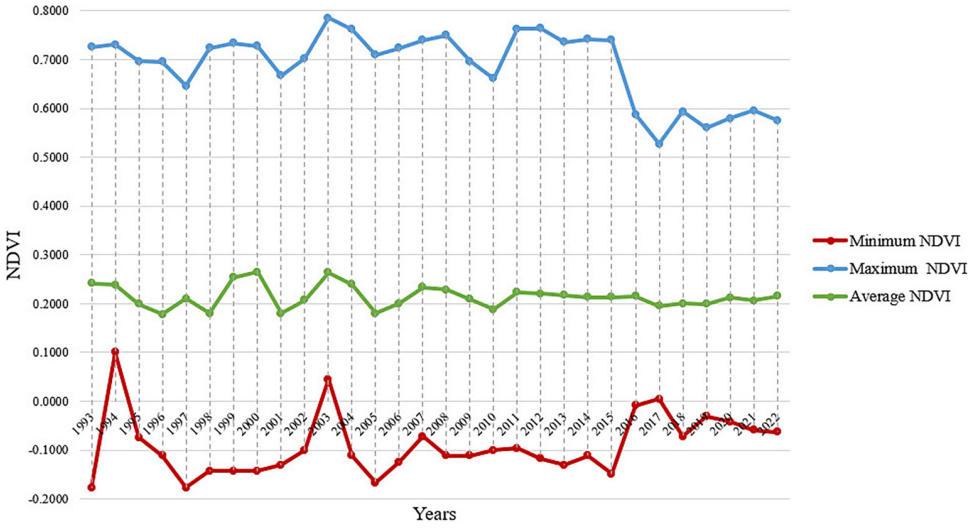

Figure 6. Minimum, maximum and average NVDI obtained from the 30-year study area

Table 1. Statistical values of the NDVI of the study area, from 1993 to 2022

Year	Minimum NDVI	Maximum NDVI	Average NDVI	Standard deviation	Satellite	Raster algorithm for obtaining NDVI	True color raster
1993	-0.18	0.73	0.24	0.14	Landsat 5	$\frac{(B4-B3)}{(B4+B3)}$	$B3+B2+B1$
1994	-0.10	0.73	0.24	0.13			
1995	-0.07	0.70	0.20	0.12			
1996	-0.11	0.69	0.18	0.11			
1997	-0.18	0.65	0.21	0.11			
1998	-0.14	0.72	0.18	0.12			
1999	-0.14	0.73	0.25	0.13			
2000	-0.14	0.73	0.27	0.13			
2001	-0.13	0.67	0.18	0.11			
2002	-0.10	0.70	0.21	0.12			
2003	0.04	0.79	0.26	0.12			
2004	-0.11	0.76	0.24	0.13			
2005	-0.17	0.71	0.18	0.14			
2006	-0.13	0.72	0.20	0.14			
2007	-0.07	0.74	0.23	0.14			
2008	-0.11	0.75	0.23	0.13			
2009	-0.11	0.70	0.21	0.13			
2010	-0.10	0.66	0.19	0.13			
2011	-0.09	0.76	0.22	0.14			
2012	-0.12	0.76	0.22	0.16			
2013	-0.13	0.74	0.22	0.14	Landsat 8	$\frac{(B5-B4)}{(B5+B4)}$	B4+B3+B2
2014	-0.11	0.74	0.21	0.13			
2015	-0.15	1.00	0.21	0.14			
2016	-0.01	0.59	0.21	0.09			
2017	0.01	0.53	0.20	0.07			
2018	-0.07	0.59	0.20	0.11			
2019	-0.03	0.56	0.20	0.09			
2020	-0.04	0.58	0.21	0.10			
2021	-0.06	0.60	0.21	0.10			
2022	-0.06	0.58	0.21	0.09			

vegetation by taking advantage of the ability of plants to emit or reflect radiation from the red and infrared bands (Perez, 2014) which is measured by several remote sensors installed on a space platform such as Landsat.

Likewise, in the Atlantic slope areas, NDVIs are high being conformed by forests with vigorous vegetation that can exceed an NDVI of 0.8 (Romero, 2016), due to the greater presence of rainfall.

CONCLUSIONS

When evaluating the normalized difference vegetation index was different from the Tayacaja valley of the department of Huancavelica-Peru; rasterizing the vector satellite map images from the year 1993 to the year 2022 using Quantum GIS, based on the red and near infrared maps, a minimum NDVI value of -0. 18, which corresponds to the aquatic body of the Upamayu River that crosses the study area from west to east; while the highest NDVI obtained was 0.79, which indicates a greater vegetation cover consisting mainly of eucalyptus plants, located to the north of the valley. Also, a mean NDVI of 30 years was determined which approximates 0.21; this is an indicator that the vegetation is scarce and in turn is decreasing mainly due to population growth. Likewise, the result of the investigation shows

that the vegetation in the valley of Tayacaja is decreasing, due to various factors, mainly anthropogenic; therefore, this valley should be reforested to improve the quality of the environment for the benefit of its population.

Acknowledgements

Thanks to the Facultad de Ingeniería Electrónica-Sistemas of the Universidad Nacional de Huancavelica for their support with computer laboratory equipment for the analysis and processing of satellite images.

REFERENCES

1. Cacilda-André, J., Lastra-Rivero, J.F., Montero, G.I. 2023. Análisis multitemporal aplicado a la gestión ambiental en la extracción de rocas y minerales industriales en Sumbe, Angola. Universidad y Sociedad, 15(S1 SE-Artículos). https://rus.ucf.edu.cu/index.php/rus/article/view/3717
2. Camas-Guardamino, D.J., Mamani-Sinche, M.S. 2022. Evaluación de la vegetación y saturación del suelo en el Área de Conservación Regional Humedales de Ventanilla mediante teledetección en Perú, 2006-2021. Revista de Ciencias Ambientales, 56(1), 54–74. https://doi.org/10.15359/rca.56/1.3
3. Carbajal Morán, H., Márquez Camarena, J.F., Zárate Quiñones, R.H., De la Cruz Vílchez, E.E. 2021. Monitoring the Hydrogen Potential of a River in the Central Andes of Peru From the Cloud. Ecological Engineering & Environmental Technology, 22(6), 17–26. https://doi.org/10.12912/27197050/141676
4. Dutta, D., Rahman, A., Paul, S.K., Kundu, A. 2021. Spatial and temporal trends of urban green spaces: an assessment using hyper-temporal NDVI datasets. Geocarto International, 1–21. https://doi.org/10.1080/10106049.2021.1989499
5. Fokeng, R.M., Fogwe, Z.N. 2022. Landsat NDVI-based vegetation degradation dynamics and its response to rainfall variability and anthropogenic stressors in Southern Bui Plateau, Cameroon. Geosystems and Geoenvironment, 1(3), 100075. https://doi.org/10.1016/j.geogeo.2022.100075f
6. Fung, T., Siu, W. 2000. Environmental quality and its changes, an analysis using NDVI. International Journal of Remote Sensing, 21(5), 1011–1024. https://doi.org/10.1080/014311600210407
7. GOREH. 2007. Estudio de diagnóstico y zonificación de la provincia de Tayacaja. Journal of Chemical Information and Modeling, 246. https://doi.org/10.1017/CBO9781107415324.004
8. Guo, E., Wang, Y., Wang, C., Sun, Z., Bao, Y., Mandula, N., Jirigala, B., Bao, Y., Li, H. 2021. NDVI indicates long-term dynamics of vegetation and its driving forces from climatic and anthropogenic factors in Mongolian Plateau. Remote Sensing, 13(4), 688. https://doi.org/10.3390/rs13040688
9. Huang, S., Tang, L., Hupy, J.P., Wang, Y., Shao, G. 2021. A commentary review on the use of normalized difference vegetation index (NDVI) in the era of popular remote sensing. Journal of Forestry Research, 32(1), 1–6. https://doi.org/10.1007/s11676-020-01155-1
10. Jia, X., Han, H., Feng, Y., Song, P., He, R., Liu, Y., Wang, P., Zhang, K., Du, C., Ge, S. 2023. Scale-dependent and driving relationships between spatial features and carbon storage and sequestration in an urban park, in Zhengzhou, China. Science of The Total Environment, 164916. https://doi.org/10.1016/j.scitotenv.2023.164916
11. Kasoro, F.R., Yan, L., Zhang, W., Asante-Badu, B. 2021. Spatial and temporal changes of vegetation cover in china based on modis ndvi. Appl. Ecol. Environ. Res, 19, 1371–1390. https://doi.org/10.15666/aeer/1902_13711390
12. Lacouture, D.L., Broadbent, E.N., Crandall, R.M. 2020. Detecting vegetation recovery after fire in a fire-frequented habitat using normalized difference vegetation index (NDVI). Forests, 11(7), 749. https://doi.org/10.3390/f11070749
13. Li, C., Jia, X., Zhu, R., Mei, X., Wang, D., Zhang, X. 2023. Seasonal Spatiotemporal Changes in the NDVI and Its Driving Forces in Wuliangsu Lake Basin, Northern China from 1990 to 2020. Remote Sensing, 15(12), 2965. https://doi.org/10.3390/rs15122965
14. Meng, N., Wang, N., Cheng, H., Liu, X., Niu, Z. 2023. Impacts of climate change and anthropogenic activities on the normalized difference vegetation index of desertified areas in northern China. Journal of Geographical Sciences, 33(3), 483–507. https://doi.org/10.1007/s11442-023 -2093-y
15. Oddi, L., Migliavacca, M., Cremonese, E., Filippa, G., Vacchiano, G., Siniscalco, C., Morra di Cella, U., Galvagno, M. 2022. Contrasting responses of forest growth and carbon sequestration to heat and drought in the Alps. Environmental Research Letters, 17(4), 45015. https://doi.org/10.1088/1748-9326/ac5b3a
16. Pérez, L. 2014. Identificación de vegetación en imágenes satelitales [Instituto Politécnico Nacional]. https://tesis.ipn.mx/bitstream/handle/123456789/18056/Identificacion de vegetacion en imagenes satelitales.pdf?sequence=1&isAllowed=y
17. Radočaj, D., Šiljeg, A., Marinović, R., Jurišić, M. 2023. State of major vegetation indices in precision agriculture studies indexed in web of science: A review. Agriculture, 13(3), 707. https://doi.org/10.3390/agriculture13030707

18. Rahman, M.M., Lamb, D.W. 2017. The role of directional LAI in determining the fAPAR–NDVI relationship when using active optical sensors in tall fescue (Festuca arundinacea) pasture. International Journal of Remote Sensing, 38(11), 3219–3235. https://doi.org/10.1080/01431161.2017.1292069
19. Ramos, A.P.M., Osco, L.P., Furuya, D.E.G., Gonçalves, W.N., Santana, D.C., Teodoro, L.P.R., da Silva Junior, C.A., Capristo-Silva, G.F., Li, J., Baio, F.H.R. 2020. A random forest ranking approach to predict yield in maize with uav-based vegetation spectral indices. Computers and Electronics in Agriculture, 178, 105791.
20. Reymundo, B.J.Q., Acevedo, R.H.R. 2020. Temperatura superficial y estado de la vegetación del bosque de Polylepis spp, distrito de San Marcos de Rocchac, Huancavelica–Perú. Enfoque UTE, 11(3), 69–86.
21. Romero, M. 2016. Evaluacion del Indice de Vegetacion de Diferencia Normalizada para determinar el estado de conservación del bosque de ceja andina sur occidental del parque nacional Sagay, Parroquia Achupallas, Canton Alaisi, provincia de Chimbotazo, 1–46. http://dspace.espoch.edu.ec/bitstream/123456789/5138/1/33T0159.pdf
22. Spadoni, G.L., Cavalli, A., Congedo, L., Munafò, M. 2020. Analysis of Normalized Difference Vegetation Index (NDVI) multi-temporal series for the production of forest cartography. Remote Sensing Applications: Society and Environment, 20, 100419. https://doi.org/10.1016/j.rsase.2020.100419
23. USGS. 2020. EarthExplorer. https://earthexplorer.usgs.gov/
24. USGS. 2021. EarthExplorer. https://earthexplorer.usgs.gov/
25. USGS. 2023a. Landsat 5, U.S. Geological Survey. https://www.usgs.gov/landsat-missions/landsat-5
26. USGS. 2023b. Landsat 8, U.S. Geological Survey. https://www.usgs.gov/landsat-missions/landsat-8
27. Xu, Z., Cao, L., Zhong, S., Liu, G., Yang, Y., Zhu, S., Luo, X., Di, L. 2020. Trends in global vegetative drought from long-term satellite remote sensing data. IEEE Journal of Selected Topics in Applied Earth Observations and Remote Sensing, 13, 815–826. https://doi.org/10.1109/JSTARS.2020.2972574.